Phonon-assisted radiative transfer*

T. Holstein, S. K. Lyo, and R. Orbach
Department of Physics, University of California, Los Angeles, California 90024
(Received 27 September 1976)

The radiative-transfer rate for inhomogeneously broadened optical lines is calculated. Photon emission and absorption is supplemented by one- and two-phonon processes to achieve energy conservation. These photon-assisted radiative transfer processes are shown to be effective at low concentrations, where electrostatic and exchange processes are weak, in the intermediate or strong radiative trapping regime. Specific application is made to the case of dilute ruby, and explicit transfer rates are calculated. The coherence factors, which undermine nonradiative single-phonon-assisted energy transfer for a small energy mismatch, are not important for radiative transfer, if the photon mean free path is longer than the wavelength of the energy matching phonon. The one-phonon process is found to vary linearly with temperature, and to be independent of the energy mismatch. However, the calculated rate for the case of ruby is found to be very slow. The two-phonon-assisted radiative-transfer process rates are calculated. They dominate the one-phonon-assisted rate for all reasonable temperatures. The results of an earlier paper are shown to be related to phonon-assisted radiative transfer if one replaces the exchange coupling between transfer sites J by $\sim\tau_R^{-1}\hbar/(r_0/\lambda)$. Here τ_R is the radiative lifetime, r_0 the distance between sites, and λ the photon wavelength involved in the radiative transfer. This replacement results in a line center to wing transfer rate equal to $1.1\times10^2\ e^{-42/T}\ \mathrm{sec}^{-1}$ for ruby (independent of concentration for a photon mean free path smaller than the sample size).

I. INTRODUCTION

We have examined phonon-assisted energy transfer in inhomogeneously broadened systems in three previous papers.[1-3] The principal coupling mechanism between transfer sites was taken to be exchange, but the method was sufficiently general to include electrostatic (e.g., quadrupole-quadrupole coupling) interactions as well. Very recent experiments at low Cr concentrations in ruby by Selzer and Yen[4] have exhibited evidence for radiative transfer. To our knowledge, there is no satisfactory treatment of phonon-assisted radiative transfer. We therefore present here a treatment of spatial energy transfer by virtue of photon emission and absorption between inhomogeneously broadened sites. One- and two-phonon processes are incorporated into the theory to make up the energy mismatch concomitant with inhomogeneous broadening.

We treat the phonons on the same basis as the photons. We showed[1,3] that this approach was the only one that could generate satisfactory transfer rates in detail, the usual lifetime broadened overlap model[5] being only approximate (and in some cases seriously misleading[6]). It will turn out that the one-phonon assisted radiative transfer process will be much too small to explain the results[4] for dilute ruby. The two-phonon-assisted radiative transfer process gives rates of about the right magnitude to explain the data.

Inherent in all of these considerations is the requirement that the sample size be large compared to the mean free path for the photon participating in the transfer process. More precisely, the active volume must be of the order of k^{-3}, where k is the absorption coefficient. Under such a condition, the probability of absorption of the photon is unity, and the energy transfer process is most efficient. For smaller volumes, the photons can "leak" out of the active volume before energy transfer occurs. In the former case, we find the energy transfer rate to be independent of concentration of the active element (for ruby, the Cr impurity). This remarkable result is a consequence of the "efficiency" of photon use in the transfer process, giving rise to a slowly decaying radial dependence (i.e., inverse square dependence on the distance) between the two sites. For smaller samples, the efficiency is reduced, the rate becomes sample shape and concentration dependent, and the transfer time is lengthened.

The lack of dependence of transfer rate on concentration (for sufficiently large samples) means that the radiative transfer rate will become important for any optical system at sufficiently low concentrations. The actual value of the cross-over concentration will depend on the mechanism for transfer at higher concentrations. It will be larger for the more rapidly varying electrostatic and exchange transfer integrals. Thus, for ruby, phonon-assisted radiative transfer appears to dominate for as high as 0.05-at.% Cr.[4]

We treat the cases of one- and two-phonon assistance separately. Section II exhibits our calculation of the one-phonon-assisted radiative-transfer rate, together with a discussion of the role of the coherence factors. We calculate two-

phonon-assisted radiative-transfer rates in Sec. III, indicating how the results of a previous paper[1] can be taken over to radiative transfer by a simple replacement of the transfer integral by (approximately) $\tau_R^{-1}\hbar/(r/\lambda)$, where τ_R is the radiative lifetime, r the distance between transfer sites, and λ the wavelength of the participating photon. We summarize our results in Sec. IV.

II. ONE-PHONON-ASSISTED RADIATIVE TRANSFER

We consider two sites, labeled 1 and 2, between which transfer is to take place. We suppose that initially site 1 is in the excited state (denoted by 1*), and site 2 in the ground state (denoted by 2). The excited state energies of sites 1, 2 (relative to the ground levels) are taken as E_1 and E_2, respectively. The optical transition energies of the two sites (the ${}^4A_2 \rightarrow \bar{E}$ transition for ruby, for example) differ by an amount $\Delta E_{12}=E_1-E_2$. The final state of the system finds site 1 in the ground level (denoted by 1), site 2 in the excited state (denoted by 2*), and a phonon of energy ΔE_{12} emitted (absorbed if ΔE_{12} is negative). Two processes are important: a phonon of energy $\hbar\omega_{\vec{q}}=\Delta E_{12}$ is emitted at site 1, a photon of wave vector $\vec{k}$ is emitted at site 1, and the same photon is absorbed at site 2; or the phonon is emitted at site 2, with the same photon emission and absorption as before. The processes are labeled (a) and (b), respectively, and are pictured in Figs. 1(a) and 1(b). Simple time-dependent perturbation theory yields the t matrix for process (a):

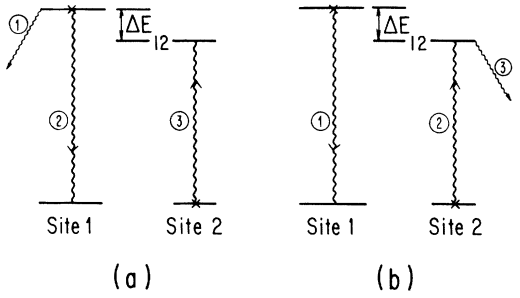

FIG. 1. One-phonon-assisted radiative transfer. The larger wiggly lines represent photons, the smaller lines phonons of wave vector $\vec{q}$ ($\hbar w_s|\vec{q}|=\Delta E_{12}$, the energy mismatch between sites 1 and 2). The circled numbers represent the position of the step in the perturbation chain. The crosses denote initial electronic occupancies, the arrows the sense of the transition. (a) A phonon of wave vector $\vec{q}$ is emitted at site 1, a photon of wave vector $|\vec{k}|=E_2/\hbar c$ [see Eq. (3)] is emitted at site 1, and the same photon is absorbed at site 2. (b) A photon of wave vector $|\vec{k}|=E_1/\hbar c$ [see Eq. (4)] is emitted at site 1, the same photon is absorbed at site 2, and a phonon of wave vector $\vec{q}$ is emitted at site 2.

$$t^{(a)}_{f\leftarrow i}=\sum_{\vec{k}}\frac{\langle n_{\vec{q}}\pm1,1,2^*|H_{\vec{k}}|n_{\vec{q}}\pm1,1,2\rangle\langle n_{\vec{q}}\pm1,1,2|H_{\vec{k}}|n_{\vec{q}}\pm1,1^*,2\rangle\langle n_{\vec{q}}\pm1,1^*,2|H(1)|n_{\vec{q}},1^*,2\rangle}{(\mp\hbar\omega_{\vec{q}})(E_2-\hbar\Omega_{\vec{k}}-i\Gamma)}. \tag{1}$$

Here, we have defined the photon energy as $\hbar\Omega_{\vec{k}}$, the electron-photon coupling Hamiltonian as $H_{\vec{k}}$, the spin-phonon coupling Hamiltonian at site 1 as $H(1)$, and taken Γ as the linewidth of the excited state (we have ignored the broadening of the ground state). The upper and lower signs correspond to phonon emission (for $\Delta E_{12}>0$) and phonon absorption (for $\Delta E_{12}<0$) processes, respectively. We make three further definitions:

$$\langle n_{\vec{q}}\pm1,1^*,2|H(1)|n_{\vec{q}},1^*,2\rangle \equiv f_1\langle n_{\vec{q}}\pm1|\epsilon|n_{\vec{q}}\rangle\exp(\mp i\vec{q}\cdot\vec{r}_1), \tag{2a}$$

$$\langle n_{\vec{q}}\pm1,1,2|H(1)|n_{\vec{q}},1,2\rangle \equiv f_0\langle n_{\vec{q}}\pm1|\epsilon|n_{\vec{q}}\rangle\exp(\mp i\vec{q}\cdot\vec{r}_1), \tag{2b}$$

and

$$\langle 1,2^*|H_{\vec{k}}|1,2\rangle\langle 1,2|H_{\vec{k}}|1^*,2\rangle \equiv F(\vec{k})\exp[i\vec{k}\cdot(\vec{r}_1-\vec{r}_2)]. \tag{2c}$$

In this notation, f_1 and f_0 are the strengths of the spin-phonon coupling constants in the excited and ground states (we assume that they are the same for all sites), and $F(\vec{k})$ the product of the electron-photon coupling constants (each proportional to $k^{-1/2}$). The former quantities (actually their difference, which will be the only important relationship for this study) can be obtained from static stress measurements.[7] The latter can be estimated from the radiative "f" number.[8] Using these definitions, and energy conservation between the final and initial states (i.e., $\mp\hbar\omega_{\vec{q}}=-E_{12}$), the "$t$" matrix, (1), can be rewritten

$$t^{(a)}_{f\leftarrow i}=\frac{f_1\langle n_{\vec{q}}\pm1|\epsilon|n_{\vec{q}}\rangle\exp(\mp i\vec{q}\cdot\vec{r}_1)}{-\Delta E_{12}}\times\sum_{\vec{k}}\frac{F(\vec{k})\exp[i\vec{k}\cdot(\vec{r}_1-\vec{r}_2)]}{E_2-\hbar\Omega_{\vec{k}}-i\Gamma}. \tag{3}$$

A similar analysis for process (b) results in

$$t^{(b)}_{f\leftarrow i}=\frac{f_1\langle n_{\vec{q}}\pm1|\epsilon|n_{\vec{q}}\rangle\exp(\mp i\vec{q}\cdot\vec{r}_2)}{\Delta E_{12}}\times\sum_{\vec{k}}\frac{F(\vec{k})\exp[i\vec{k}\cdot(\vec{r}_1-\vec{r}_2)]}{E_1-\hbar\Omega_{\vec{k}}-i\Gamma}. \tag{4}$$

The above two processes refer to phonon emission or absorption in the excited level. In addition, phonon emission or absorption can equally well occur in the ground level. The effect of adding these diagrams to Figs. 1(a) and 1(b) is to simply replace f_1 in (3) and (4) by $f_1 - f_0$ (because of differing signs of the energy denominators). We shall make this replacement in subsequent equations [e.g., Eq. (10) below].

We proceed to examine the two sums appearing in (3) and (4). To obtain a dimensionless form, we define $\vec{r} = \vec{r}_1 - \vec{r}_2$, and

$$k_1 = E_1/\hbar c, \quad \kappa_1 = k_1 r,$$

$$k_2 = E_2/\hbar c, \quad \kappa_2 = k_2 r, \quad F(\vec{k}) = F_0 k^{-1},$$

with F_0 independent of $\vec{k}$. The sum in (4), for example, can be represented by an effective exchange coupling (by comparison with Refs. 1–3),

$$J_1^{\text{eff}}(E_1, r) = (VF_0/2\pi\hbar c r) I(\kappa_1), \tag{5}$$

with

$$I(\kappa_1) = \frac{1}{\pi}\int_0^\infty d\kappa \, \frac{\sin\kappa}{\kappa_1 - \kappa - i\Gamma r/\hbar c}. \tag{6}$$

Here, V is the active volume of the crystal. In general, at low temperatures Γ is sufficiently small that the last term in the denominator of (6) is much smaller than one. That is, for ruby at conventional temperatures, $\Gamma/hc \ll 1$ cm^{-1}. For Γ/hc equal to 1 cm^{-1}, $\Gamma r/\hbar c = 7r$, where r is measured in cm. It will turn out that energy transfer will be important between sites separated by no more than a mean free path for the photon. For sensible concentrations of Cr in ruby, this will imply r's of the order of hundreds of microns, so that indeed $\Gamma r/\hbar c \ll 1$. At low temperatures, Γ is exponentially small[9] and substantially larger values of r result in the same inequality. Under this condition, $I(\kappa_1)$ becomes[10]

$$I(\kappa_1) = (1/\pi)\sin\kappa_1 \,\mathrm{ci}(\kappa_1) - \cos\kappa_1[(1/\pi)\,\mathrm{si}(\kappa_1) + 1] + i\sin\kappa_1, \tag{7}$$

where

$$\mathrm{si}(\kappa_1) = -\int_{\kappa_1}^\infty \frac{\sin t}{t}dt; \quad \mathrm{ci}(\kappa_1) = -\int_{\kappa_1}^\infty \frac{\cos t}{t}dt. \tag{8}$$

The asymptotic properties of these functions are[10]

$\kappa_1 \ll 1$, $\mathrm{si}(\kappa_1) \simeq -\frac{1}{2}\pi + \kappa_1$,
$\mathrm{ci}(\kappa_1) \simeq -\ln(1/\gamma\kappa_1)$ (γ is Euler's constant);

$\kappa_1 \gg 1$, $\mathrm{si}(\kappa_1) \simeq -\cos\kappa_1/\kappa_1$,
$\mathrm{ci}(\kappa_1) \simeq \sin\kappa_1/\kappa_1$.

These properties result in

$$\kappa_1 \ll 1, \quad I(\kappa_1) \simeq -\tfrac{1}{2}; \tag{9a}$$

$$\kappa_1 \gg 1, \quad I(\kappa_1) \simeq -e^{-i\kappa_1}. \tag{9b}$$

For ruby, where $E_1 = 14\,400$ cm^{-1}, the inequality (9a) is equivalent to $r \ll 1000$ Å, while (9b) corresponds to $r \gg 1000$ Å.

The two processes, (a) and (b), involve different photon energies. This can be seen from the Green's functions exhibited in Eqs. (3) and (4). Process (a) involves a photon of energy E_2; process (b) a photon of energy E_1. Because of trapping, it may turn out that only one of the two photons is effective in energy transport (see discussion below). Hence, it will be necessary to keep the "t" matrices separate for processes (a) and (b).

The transition probability per unit time for energy transfer between site 1 and 2 is given by

$$W_{2\leftarrow 1} = \frac{2\pi}{\hbar}\sum_{\vec{q}} |t_{f\leftarrow i}|^2 \delta(\hbar\omega_{\vec{q}} \mp \Delta E_{12}), \tag{10}$$

where the sum over phonon momenta $\vec{q}$ includes the sum over phonon polarizations, and the $-$ ($+$) sign refers to phonon emission (absorption) in the energy transfer process. When (3) and (4) are inserted in (10), there will be a cross term in addition to the absolute squares. This cross term will involve both photons (of energy E_1 and E_2) and also a phase factor $e^{\pm i\vec{q}\cdot\vec{r}}$. This term is the origin of an interference[3] arising from the one-phonon emission or absorption on one site interfering with the identical process on the other site. We discuss in Ref. 3 how this interference term reduces the importance of one-phonon-assisted energy transfer in the case of electrostatic or exchange couplings. For one-phonon-assisted photon exchange, however, $|\vec{r}|$ can vary over very large distances, of the order of the mean free path for photon absorption. The δ function in (10) restricts the phonon wave vector to $|\vec{q}| = \Delta E_{12}/\hbar v_s$, where v_s is the phonon velocity. For dilute ruby, $\Delta E_{12} \simeq 0.1$ cm^{-1}, whence $|\vec{q}| = 1.8\times 10^{-4}$ Å^{-1}. Phonon-assisted photon exchange takes place over distances of the order of hundreds of microns in dilute ruby, so that typically $\vec{q}\cdot\vec{r} \gg 1$ (the number of sites increasing as r^3). Hence, the long mean free path of the photons, compared to the phonon wavelength, averages the interference term to zero. The inclusion of (3) and (4) in (10) therefore involves only the absolute square of the respective "t" matrices. This allows us to separate our consideration of each photon, or energy E_1 or E_2, in the transfer process.

We show in the Appendix that

$$|J_1^{\text{eff}}(E_1, r)| = \tau_R^{-1}\hbar\,|I(\kappa_1)|/2\kappa_1 \sim \tau_R^{-1}\hbar/(r/\lambda), \tag{11}$$

where τ_R is the radiative lifetime and λ the photon wavelength. For ruby, $\tau_R \simeq 3.6$ msec is the radiative "R_1" lifetime for transitions between the $\bar{E}$ and the $^4A_2$ levels, and $\lambda \sim 6800$ Å.

Inserting (11) and (5) in (4), and an analogous expression for the photon of energy E_2 in (3), and using (10), we obtain the transition probabilities per unit time for energy transfer between sites 1 and 2 for each of the photons:

$$W_{2\leftarrow 1}(E_2) = \frac{2\pi}{\hbar}\frac{(\tau_R^{-1}\hbar)^2}{2(\Delta E_{12})^2}\frac{|I(\kappa_2)|^2}{(2\kappa_2)^2}(f_1-f_0)^2 \times \sum_{\vec{q}} |\langle n_{\vec{q}}^{+} \pm 1|\epsilon|n_{\vec{q}}^{+}\rangle|^2 \delta(\hbar\omega_{\vec{q}}^{+} \mp \Delta E_{12}); \tag{12a}$$

$$W_{2\leftarrow 1}(E_1) = \frac{2\pi}{\hbar}\frac{(\tau_R^{-1}\hbar)^2}{2(\Delta E_{12})^2}\frac{|I(\kappa_1)|^2}{(2\kappa_1)^2}(f_1-f_0)^2 \times \sum_{\vec{q}} |\langle n_{q} \pm 1|\epsilon|n_{\vec{q}}^{+}\rangle|^2 \delta(\hbar\omega_{\vec{q}}^{+} \mp \Delta E_{12}). \tag{12b}$$

Rather than evaluate the phonon sum in (12) explicitly, it is simpler for the case of ruby, and more illuminating, to express $W_{2\leftarrow 1}$ in terms of the phonon-induced transition rate between the $\bar{E}$ and $2\bar{A}$ levels. This rate is known from excited-state electron-spin resonant measurements,[11] as interpreted by Ref. 9. One knows that

$$W_{2\bar{A}\leftarrow\bar{E}} = \frac{2\pi}{\hbar}\sum_{\vec{q}} |\langle 2\bar{A}, n_{\vec{q}}^{+} - 1|H|\bar{E}, n_{\vec{q}}^{+}\rangle|^2 \delta(\hbar\omega_{\vec{q}}^{+} - \delta) \equiv \frac{2\pi}{\hbar}\sum_{\vec{q}} A^2 |\langle n_{\vec{q}}^{+} - 1|\epsilon|n_{\vec{q}}^{+}\rangle|^2 \delta(\hbar\omega_{\vec{q}}^{+} - \delta), \tag{13}$$

defining the "off diagonal" phonon coupling constant A. This quantity can be obtained in the long-wavelength limit from the static stress data of Schawlow.[7] The energy δ in (13) is the ^2E splitting (29 cm^{-1}). We shall assume little dispersion in the phonon spectrum between energies on the scale of ΔE_{12} and δ. Assuming a Debye spectrum, and dividing (12b) by (13), we obtain

$$\frac{W_{2\leftarrow 1}(E_1)}{W_{2\bar{A}\leftarrow\bar{E}}} = \frac{(\tau_R^{-1}\hbar)^2}{2(\Delta E_{12})^2}\frac{|I(\kappa_1)|^2}{(2\kappa_1)^2} \times \left(\frac{f_1-f_0}{A}\right)^2 \frac{|\Delta E_{12}|^3}{\delta^3 n(\delta)} \begin{Bmatrix} n(|\Delta E_{12}|)+1 \\ n(|\Delta E_{12}|) \end{Bmatrix}, \tag{14}$$

with an analogous expression for $W_{2\leftarrow 1}(E_2)$ obtained by substitution of κ_2 for κ_1 in (14).

Here, $n(x)$ is the Bose factor, $n(x) = (e^{x/k_BT} - 1)^{-1}$. The two choices in curly brackets depend on whether the phonon of energy ΔE_{12} is emitted or absorbed in the energy-transfer process. For the case of ruby $\Delta E_{12} \ll k_BT$, and (14) can be substantially simplified. Using the experimental value[9,11]

$$W_{2\bar{A}\leftarrow\bar{E}} = 3\times 10^9 n(\delta)\ \text{sec}^{-1},$$

we obtain

$$W_{2\leftarrow 1}(E_1) = (\tau_R^{-1}\hbar)^2 \frac{|I(\kappa_1)|^2}{2(2\kappa_1)^2}\left(\frac{f_1-f_0}{A}\right)^2 \frac{k_BT}{\delta^3} \times 3\times 10^9\ \text{sec}^{-1}, \tag{15}$$

with an analogous expression for $W_{2\leftarrow 1}(E_2)$ given by replacing κ_1 by κ_2 in (15). The difference between κ_1 and κ_2 lies in the energy mismatch ΔE_{12}. Because $\Delta E_{12}/E_1 \ll 1$, one has $\kappa_1 \simeq \kappa_2$, and therefore $W_{2\leftarrow 1}(E_1) \simeq W_{2\leftarrow 1}(E_2)$.

One of the nice features of (15) is the appearance of the ratio $(f_1-f_0)/A$. The static strain measurements of the R_1 and R_2 energies give this ratio directly for ruby, with no analysis required. Note also that (15) is independent of the energy mismatch ΔE_{12}, and linearly dependent on the temperature, as is the usual result for one-phonon-assisted energy transfer when the temperature is higher than the energy mismatch.[8]

The expression (15) applies to the energy transfer between two given sites via the energy-transfer process (b). It is the rate assuming that site 1 has an optical splitting E_1 and site 2 has an optical splitting E_2. In order to relate the above two-site jump rate to the experimentally observable spectral diffusion rate, we designate $W_{E_i}(E_2-E_1)$ as the total spectral diffusion rate from an initial line at E_1 to a final line at E_2 via a photon of energy $E_i (i=1,2)$. This rate can be found by summing (15) over all sites within a volume characterized by the mean free path for photon E_1, $l(E_1)$. One has

$$W_{E_1}(E_2-E_1) = \sum_{2} W_{2\leftarrow 1}(E_1) = \int_0^{l(E_1)} W_{2\leftarrow 1}(E_1)\, 4\pi r^2 n\, dr, \tag{16}$$

where n is the impurity density. We are implicitly assuming that the sample dimensions are larger than the mean free path for photon E_1. If the reverse is true, the integration must be truncated by the sample boundaries, and the rate $W_{E_1}(E_1-E_2)$ becomes sample size (and shape) dependent. The total rate is given by

$$W(E_2-E_1) = \sum_{i=1,2} W_{E_i}(E_2-E_1).$$

If $l(E_2) \sim l(E_1)$, then $W_{E_1}(E_2-E_1) \sim W_{E_2}(E_2-E_1)$.

An explicit value for $l(E_1)$ can be found from standard considerations,[12]

$$l(E_1)^{-1} = \tfrac{1}{2}\pi n\lambda^2\, g(E_1)/\tau_R\,, \tag{17}$$

where $g(E_1)$ is the equilibrium inhomogeneously broadened line shape at energy E_1. For the case of dilute ruby, $g(E_1)\sim(0.1\ \mathrm{cm}^{-1})^{-1}$ at the line center, whence $l(E_1) = 3.8\times10^{17}/n$. For 0.1 at.% ($n = 10^{19}$), this leads to $l(E_1) = 0.038$ cm. This value serves as the justification for our previous remark that the photon mean free path is much larger than the wavelength of the phonon involved in making up the energy mismatch ΔE_{12}. Because the upper limit in (16) is so large, we are in the limit of (9b) for $I(\kappa_1)$. We insert (9b) into (15), and carry out the integration (16). We obtain

$$W_{E_1}(E_2-E_1) = (\tau_R^{-1}/\hbar)^2[(f_1-f_0)/A]^2(k_BT/2\delta^3) \times 3\pi\times10^9[nl(E_1)/k_1^2]\ \mathrm{sec}^{-1}. \tag{18}$$

But the factor in the last square bracket equals $(2/\pi)\tau_R/g(E_1)$. We thereby arrive at the remarkable result that $W_{E_1}(E_1-E_2)$ is independent of the Cr concentration n. This result is no longer valid if the sample size is smaller than $l(E_1)$, but we have assumed moderate to strong trapping [e.g., Eq. (16)] so that the reverse is true. The independence on concentration is a direct result of the fact that the mean free path for photon E_1 diminishes as the concentration n increases, the net effect being a cancellation of the concentration dependence.

According to the static strain data,[7] $(f_1-f_0)/A \simeq 4$. Using all the parameters known for dilute ruby [i.e., $\tau_R\simeq3.6$ msec, $\delta = 29\ \mathrm{cm}^{-1} = 42$ K, $g(E_1) \simeq(0.1\ \mathrm{cm}^{-1})^{-1}\simeq0.1$ at.% of Cr], we finally reduce (18) to

$$W_{E_1}(E_2-E_1) = 2.2\times10^{-4}\ T\,\mathrm{sec}^{-1}\ \ (T\text{ in K}). \tag{19}$$

This rate is much too slow to be observed in ruby. We shall show in Sec. III that two-phonon-assisted photon exchange energy-transfer processes give much larger rates and are probably observable in ruby. The reason for the difference between one- and two-phonon assistance rates lies in the much larger density of states available to phonons of energy k_BT (involved in the two-phonon-assisted processes) than to those of energy ΔE_{12} (involved in the single-phonon-assisted processes).

Before going on to the case of two-phonon-assisted photon exchange, it is interesting to return to the calculation of the transfer rate (16). Clearly this is a rough approximation, and serves only to give an estimate for the total one-phonon-assisted energy-transfer rate [as exhibited in Eq. (19), for example]. The more correct procedure to follow in an energy-transfer calculation is to consider the energy transport equation utilizing both processes (a) and (b). The difficulty lies with the upper limit for the transfer rate [e.g., see Eq. (16)]. The transport equation will involve frequencies over a large spectral range, causing $l(E)$ to vary strongly. In general, the problem is a complicated one, but a strong simplification can be made in the case of a Gaussian form for $g(E)$.[13] In such a case, it is possible to define a cutoff energy (relative to the line center, E_c) E_0, such that photons with energy less than E_c-E_0, or energy greater than E_c+E_0 are not trapped, but are able to transverse the sample freely. The condition which fixes E_0 is simply $l(E_c+E_0) = l(E_c-E_0) = d$, the dimension of the sample. Even this condition is only approximate, as one should correctly take into account the spatial position of the emitting and absorbing sites relative to the sample boundaries. We are assuming that the spatial excitation distribution is essentially uniform. This will give us a qualitative feel for the emission profile, but will not be numerically correct.[14]

Let the emission probability function be denoted by $P(E,t)$, where t is the time. {Note that this definition [as well as that used in Eq. (1) of Ref. 2] differs from that of Motegi and Shionoya[15] in that we absorb the line-shape factor $g(E)$ into the emission probability function, whereas they do not.} Define the quantity $W(E'-E) = W_{E'}(E'-E) + W_E(E'-E)$. Then the analogy to the Motegi-Shionoya[15] equation for radiative transfer is (we measure all energies relative to the line center E_c)

$$\frac{dP(E,t)}{dt} = -\int_{-E_0}^{E_0} W_{E'}(E'-E)g(E')P(E)\,dE' - \int_{-\infty}^{\infty} W_E(E'-E)g(E')P(E)\Theta(E_0-|E|)\,dE' - \tau^{-1}(E)P(E)\mathcal{S}(E) + \int_{-\infty}^{\infty} W_E(E-E')g(E')P(E')\Theta(E_0-|E|)\,dE' + \int_{-E_0}^{E_0} W_{E'}(E-E')g(E')P(E')\,dE'\,. \tag{20}$$

The quantity $\mathcal{S}(E)$ is the "escape factor," approximately equal to unity for $|E|>E_0$, and of the order of the ratio of phonon side band emission intensity to the zero-phonon emission intensity for $|E|<E_0$. The function $\Theta(x)$ is zero if $x<0$, and 1 for $x>0$. The expression (20) for the time development of the emission probability makes a sharp distinction between photons with absolute energies less than E_0 (trapped), and those with energies greater than E_0 (escaping). This distinction is incorrect for a Lorentzian line shape, and the problem becomes much more complex. We leave the details

for a future publication.

Approximately, the trapped radiation is quenched by a factor $e^{-x/l(E)}$, where x is the distance from the sample surface. As a consequence, to an observer outside of the sample, the emitted radiation profile has the form

$$I(E)=\tau_R^{-1}[P(E,t)l(E)/d][1-e^{-d/l(E)}]\,.$$

The factors multiplying $\tau_R^{-1}P(E)$ arise from the integration of $e^{-x/l(E)}$ over x. Because $l(E)\propto g(E)^{-1}$, the product $P(E,t)l(E)$ is actually independent of $g(E)$. In the limit of large thickness the emitted radiation will have a rectangular shape.

Unfortunately, we are unable to solve (20) analytically. One must resort to a numerical integration and iteration solution of the integral equation, much as was done in Refs. 2 and 3. We reserve such a treatment for a future publication. For the present, we have outlined an approximate form for the transport equation, which must be used if one wishes to obtain the time development of the explicit emission profile. The numerical result (19) is only an estimate of the total transfer rate caused by one-phonon-assisted radiative transfer.

We now go on to treat two-phonon-assisted radiative transfer. We shall again generate an estimate of the total transfer rate. The reader is warned that an accurate treatment again requires solution of the transport equation for two-phonon-assisted radiative transfer, similar in form to (20).

III. TWO-PHONON-ASSISTED RADIATIVE TRANSFER

There are three processes which are expected to be important for two-phonon-assisted radiative transfer. The resonant component (see Ref. 1) is pictured in Figs. 2(a)–2(c). In these transfer processes, the phonon connecting the $\bar{E}$ with the $2\bar{A}$ has exactly the ^2E splitting energy δ. The t matrix for the transfer process pictured in Fig. 2(a) [in a shortened notation compared to Eq. (1)] is given by

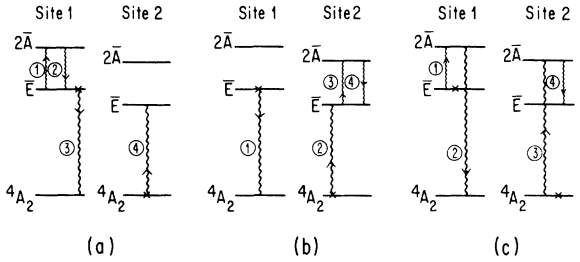

FIG. 2. Resonant two-phonon-assisted radiative transfer, as applied to ruby. The larger wiggly lines represent photons, the smaller lines phonons. The absorbed phonon has energy δ, the R_1, R_2 line splitting (the energy difference between the $\bar{E}$ and $2\bar{A}$ excited levels) and the difference in phonon energies equals the energy mismatch between sites 1 and 2. The circled numbers represent the position of the step in the perturbation chain. The crosses denote initial electronic occupancies, the arrows the sense of the transition. (a) A resonant phonon of energy δ is absorbed at site 1, another phonon is emitted at site 1, a photon of wave vector $|\vec{k}|=E_2/\hbar c$ [see Eq. (22)] is emitted at site 1, and the same photon is absorbed at site 2. (b) A photon of wave vector $|\vec{k}|=E_1/\hbar c$ [see Eq. (23)] is emitted at site 1, the same photon is absorbed at site 2, a resonant phonon of energy δ is absorbed at site 2, and another phonon is emitted at site 2. (c) A resonant phonon of energy δ absorbed at site 1, a photon of wave vector $|\vec{k}|=(E_1+\delta)/\hbar c$ [see Eq. (25)] is emitted at site 1, the same photon is absorbed at site 2, and another phonon is emitted at site 2.

$$t_{f\leftarrow i}^{(2a)}=\sum_{\vec{k}}\frac{\langle 2^*|H_{\vec{k}}|2\rangle\langle 1|H_{\vec{k}}|1^*\rangle\langle\bar{E},n_{\vec{q}'}+1|H(1)|2\bar{A},n_{\vec{q}'}\rangle\langle 2\bar{A},n_{\vec{q}}-1|H(1)|\bar{E},n_{\vec{q}}\rangle}{[-\delta+\hbar\omega_{\vec{q}}-i\Gamma(2\bar{A})][-\Delta E_{12}-i\Gamma(\bar{E})][E_1-\Delta E_{12}-\hbar\Omega_{\vec{k}}-i\Gamma(\bar{E})]}\,. \tag{21}$$

In the perturbation chain, we have taken the initial energy to equal E_1; the first intermediate energy $E_1+\delta-\hbar\omega_{\vec{q}}+i\Gamma(2\bar{A})$; the second intermediate energy $E_1-\hbar\omega_{\vec{q}}+\hbar\omega_{\vec{q}'}+i\Gamma(\bar{E})$; the third intermediate energy $-\hbar\omega_{\vec{q}}+\hbar\omega_{\vec{q}'}+\hbar\Omega_{\vec{k}}$; and the final energy to equal $-\hbar\omega_{\vec{q}}+\hbar\omega_{\vec{q}'}+E_2$ (which of course must equal E_1). We have ignored the width of the ground level. We use the definition of $J_1^{\rm eff}$ [Eqs. (5) and (6)] to simplify (21):

$$t_{f\leftarrow i}^{(2a)}=\frac{J_1^{\rm eff}(E_2,r)}{-\Delta E_{12}}\,\frac{\langle\bar{E},n_{\vec{q}'}+1|H(1)|2\bar{A},n_{\vec{q}'}\rangle\langle 2\bar{A},n_{\vec{q}}-1|H(1)|\bar{E},n_{\vec{q}}\rangle}{-\delta+\hbar\omega_{\vec{q}}-i\Gamma(2\bar{A})}\,. \tag{22}$$

We have dropped the factor $i\Gamma(\bar{E})$ as compared to ΔE_{12}, as it will be small in the temperature range where the resonant transfer processes dominate. A similar expression is easily derived for process (2b):

$$t_{f\leftarrow i}^{(2b)}=\frac{J_1^{\rm eff}(E_1,r)}{\Delta E_{12}}\,\frac{\langle\bar{E},n_{\vec{q}'}+1|H(2)|2\bar{A},n_{\vec{q}'}\rangle\langle 2\bar{A},n_{\vec{q}}-1|H(2)|\bar{E},n_{\vec{q}}\rangle}{\Delta E_{12}-\delta+\hbar\omega_{\vec{q}}-i\Gamma(2\bar{A})}\,. \tag{23}$$

For small energy mismatches, $\Delta E_{12}/k_BT\ll 1$. Using this approximation, and the argument following (15) which showed that $J_1^{\rm eff}(E_1,r)\simeq J_1^{\rm eff}(E_2,r)$, we may combine (22) and (23) to obtain

$$t_{f\leftarrow i}^{(2a)}+t_{f\leftarrow i}^{(2b)}=-\frac{J_1^{\rm eff}(E_1,r)}{\Delta E_{12}}\,\frac{|A|^2\langle n_{\vec q'}+1\,|\,\epsilon\,|\,n_{\vec q'}\rangle\langle n_{\vec q}-1\,|\,\epsilon\,|\,n_{\vec q}\rangle\, e^{-i(\vec q-\vec q')\cdot\vec r_1}}{-\delta+\hbar\omega_{\vec q}-i\Gamma(2\bar A)}\,(1-e^{i(\vec q-\vec q')\cdot\vec r}) \tag{24}$$

where we have introduced the off-diagonal phonon coupling constant A [see Eq. (13)].

The t matrix for the resonant part of the process pictured in Fig. 2(c) is given by

$$t_{f\leftarrow i}^{(2c)}=J_2^{\rm eff}(E_1+\delta,r)\,\frac{\langle n_{\vec q'}+1\,|\,\epsilon\,|\,n_{\vec q'}\rangle\langle n_{\vec q}-1\,|\,\epsilon\,|\,n_{\vec q}\rangle\exp[-i(\vec q\cdot\vec r_1-\vec q'\cdot\vec r_2)]}{[-\delta+\hbar\omega_{\vec q}-i\Gamma(2\bar A)][\Delta E_{12}-\delta+\hbar\omega_{\vec q}-i\Gamma(2\bar A)]}\,, \tag{25}$$

where J_2 relates to photon matrix elements between the $2\bar A$ and the ground $^4A_2$ level. Thus,

$$J_2^{\rm eff}(E_1+\delta,r)=\tau_{R_2}^{-1}\hbar\,|\,I(\kappa_3)|\,/2\kappa_3\,, \tag{26}$$

where the subscript R_2 on τ means the R_2 radiative lifetime. Because $\kappa_3=\kappa_1(1+\delta/E_1)$, and $E_1\gg\delta$, one has $\kappa_3\simeq\kappa_1$.

The resonance character of the denominators in (24) and (25) ensures that the phonon energies are in the vicinity of δ. This implies phonon wave vectors q and q' of the order of 10^7 cm^{-1}. When multiplied by a characteristic separation distance of $l\simeq0.01$ cm, we have the strong inequality $qr\simeq q'r\gg1$. This allows us to ignore the cross terms in the coherence factors.

The total transition probability per unit time for the resonant part of the two-phonon-assisted radiative energy transfer between site 1 and site 2 is given by the "golden rule," using (24) and (25). We find

$$\begin{aligned}W_{2\leftarrow1}^{(\rm res)}&=2\left(|J_1^{\rm eff}(E_1,r)|^2+\frac{(\Delta E_{12})^2\,|J_2^{\rm eff}(E_1+\delta,r)|^2}{(\Delta E_{12})^2+\Gamma^2(2\bar A)}\right)\frac{W_{\bar E\to2\bar A}}{(\Delta E_{12})^2}\\&=2\left[\left((\tau_{R_1}^{-1}\hbar)^2+\frac{(\Delta E_{12})^2(\tau_{R_2}^{-1}\hbar)^2}{(\Delta E_{12})^2+\Gamma^2(2\bar A)}\right)\frac{W_{\bar E\to2\bar A}}{(\Delta E_{12})^2}\right]\frac{|I(\kappa_1)|^2}{(2\kappa_1)^2}\end{aligned} \tag{27}$$

using (11). We have designated the radiative lifetime of the $\bar E$ as τ_{R_1}.

We have not separated out the individual contributions in (27) due to processes involving photons of energies E_1, E_2, $E_1+\delta$ and $E_2+\delta$, as was done in Sec. II. There are no cross terms in the coherence factors, as discussed above, so that the first (last) two processes involving photons of energy E_1, E_2 $(E_1+\delta, E_2+\delta)$ contribute equally to the first (second) term in (27). The full transport equation [see Eq. (20)] requires such a separation. However, as explained in Sec. II, we are seeking in this paper only to estimate the total phonon-assisted radiative-transfer rate. Detailed treatment of the transport equation, required for a satisfactory expression for the time development of the spectral emission profile, is beyond the scope of this work and is reserved for a future publication. In the absence of such a treatment, the results of this section should be regarded only as an estimate of the total spectral transfer rate.

The form of (27) is interesting because it is strongly suggestive of Eq. (1) in Ref. 1. That is, the quantity $(\tau_{R_1}^{-1}\hbar)I(\kappa_1)/2\kappa_1$ plays the role of the exchange coupling J_1 appropriate to the case of non-radiative-transfer. We shall exploit this result shortly when we consider the remainder of the two-phonon-assisted radiative energy-transfer processes.

In order to estimate the total two-phonon-assisted radiative-transfer rate, we make the assumption that the mean free path $l(E)$ for each of the photons involved in (27) is the same. We then carry out the integration over the volume in the same manner as in (16). Using (17), we obtain

$$W_{\rm res}(E_2-E_1)=\frac{4}{\pi}\left((\tau_{R_1}^{-1}\hbar)(\hbar\Delta\nu_1)+\frac{(\Delta E_{12})^2(\tau_{R_2}^{-1}\hbar)(\hbar\Delta\nu_2)}{(\Delta E_{12})^2+\Gamma^2(2\bar A)}\right)\frac{W_{\bar E\to2\bar A}}{(\Delta E_{12})^2}\,. \tag{28}$$

We have designated $1/g(E)$ for the R_1 and R_2 lines by $\Delta\nu_1$ and $\Delta\nu_2$, respectively.

It is interesting to explore the magnitude of (28). For dilute ruby, we take (as before) $\Delta E_{12}\sim\hbar\Delta\nu_1\sim0.1$ cm^{-1} and $\tau_{R_1}^{-1}\hbar=1.5\times10^{-9}$ cm^{-1} (for $\tau_{R_1}\simeq3.6$ msec). Taking the second term in the large parentheses of (28) equal to the first, we obtain

$$W_{\rm res}(E_2-E_1)=1.1\times10^2e^{-42/T}\ \text{sec}^{-1}. \tag{29}$$

This value is sufficiently large to be observable, and preliminary evidence[4] suggests it is about right for ruby.

Note that (28) is explicitly independent of Cr concentration. This is again because of the use of the photon mean free path l to determine the number of participating sites (exactly as in the case of single-phonon-assisted radiative transfer treated in Sec. II). There is an implicit effect of concentration in that $\Delta\nu$ will increase as the concentration increases. This is a secondary effect, however, and can easily be taken into account.

In addition to $W_{\rm res}$, Ref. 1 exhibits energy trans-

fer rates for a nonresonant process involving electronic transitions, (a) between the $\bar{E}$ and the $2\bar{A}$; (b) within the $\bar{E}$ but phonon absorption and emission on different sites; and (c) within the $\bar{E}$ and for phonon absorption and emission on the same site. These processes can all be carried over to radiative transfer as treated in this paper by simply replacing the exchange coupling J_1 of Ref. 1 by $J_1^{\text{eff}}(E,r)$ of this paper [see Eq. (11)]. This is allowable because $J_1^{\text{eff}}(E,r)$ is a very weak function of E, on the scale of k_BT, for large values of E_1. In addition, the spectral diffusion rate for radiative transfer involves sites interacting over distances of order l, so that qr and $q'r \gg 1$ ($r \sim l$, $q, q' \sim k_BT/\hbar v_s$). The interference terms of Ref. 1, therefore, do not play a role. All of the energy dependences of Ref. 1, and the relative magnitudes of the various transfer rates, also go over directly to the case of radiative transfer. As a consequence, the resonant part of the two-phonon-assisted radiative-transfer rate dominates in the helium temperature regime and above.

The two-phonon-assisted radiative-transfer rates are all explicitly independent of concentration (except for the implicit effect of concentration on the inhomogeneous linewidth $\Delta\nu$, as previously noted). However, the two-phonon-assisted non-radiative-transfer rates exhibited in Ref. 1 all increase rapidly as the concentration increases because of the rapid increase of the exchange coupling with decreasing Cr-Cr distance. One expects, therefore, to observe two-phonon-assisted radiative transfer at low concentrations, with non-radiative-transfer taking over as the concentration is increased (even though the photon trapping becomes more severe as concentration increases). The "catch" is that the concentration must not be too low, for then the photon mean free path $l(E)$ will become larger than the sample dimensions d for most if not all of the spectral line. This condition violates our assumption of moderate to strong trapping, making the use of a uniform spatial excitation distribution questionable indeed. The photons will escape from the sample, and the over-all "efficiency" of radiative transfer will sharply diminish. A simple test for this condition is the observation of a shape or sample volume dependence of the spectral transfer rate. Effects of this sort have been observed for 0.05% ruby.[4]

IV. SUMMARY AND CONCLUSIONS

We have calculated the one-phonon- and two-phonon-assisted radiative-transfer rates for an inhomogeneously broadened spectral line. We have shown that both rates are independent of concentration when the sample dimensions substantially exceed the mean free path for photon absorption (moderate to strong trapping). The one-phonon-assisted radiative transfer was shown to increase linearly with temperature, with a magnitude proportional to the inverse square of the radiative lifetime. An explicit evaluation of the transfer rate for ruby showed this process to be unimportant for that case.

The two-phonon-assisted radiative-transfer rate was calculated. When applied to ruby, the resonant part was shown to vary exponentially with $1/T$, and yield a magnitude of the order of 25 msec at 42 K according to (29). This is sufficiently large to be observable. The nonresonant two-phonon-assisted radiative-transfer processes were shown to follow from previous work on non-radiative-transfer by the replacement of the exchange coupling with the quantity $\tau_R^{-1}\hbar\,|I(\kappa_1)|\,/2\kappa_1 \sim \tau_R^{-1}\hbar/(r/\lambda)$. The relative importance of the various processes is the same as outlined previously for non-radiative-transfer (Ref. 1). The resonant process should dominate at low temperatures, while the nonresonant processes will become important above the liquid-helium temperature range.

The energy mismatch (ΔE_{12}) dependence of the radiative transfer rates are identical to the non-radiative-transfer rates of Ref. 1. The spectral diffusion treatments of Refs. 2 and 3 can therefore be taken over to the case of radiative transfer immediately.

Clearly, a systematic study of spatial-spectral diffusion in inhomogeneously broadened systems is called for. We predict that, as a function of concentration, phonon-assisted radiative transfer should dominate at low concentrations, with non-radiative-transfer becoming important as the concentration is increased. The former rate may be sample shape and/or volume dependent if the photon mean free path exceeds the sample dimensions.

Though we have applied our results exclusively to the case of dilute ruby, they are relevant to a wide variety of physical systems (e.g., the rare-earth-doped glasses[16]). Different spectral level structures may lead to differences in the relative importance of phonon-assisted resonant and non-resonant-transfer rates.

Finally, we emphasize that our calculations are only estimates of the total phonon-assisted radiative-transfer rates. A proper treatment must include the spatially-dependent transport equation. Even if the spatial excitation distribution is taken as uniform [an approximation which requires $l(E) \ll d$, where d is a characteristic crystal dimension], the time development of the emission profile requires solution of a complicated diffusion equation [e.g., Eq. (20)]. Our results, therefore [e.g., Eqs. (19) and (29)], are only approximate

estimates of the total transfer rate. A full treatment is reserved to a future publication.

ACKNOWLEDGMENT

We wish to acknowledge very valuable discussions with Dr. P. M. Selzer. He first suggested to us the importance of phonon-assisted radiative transfer and assisted us in understanding the temperature and concentration regimes where it would be expected to contribute significantly.

APPENDIX A

According to (2c) and (5),

$$|J_1^{\rm eff}(E_1,r)| = [V\kappa_1 I(\kappa_1)/2\pi\hbar c r^2] \times |\langle 1,2^*|H_{\vec{k}}|1,2\rangle\langle 1,2|H_{\vec{k}}|1^*,2\rangle| . \tag{A1}$$

We shall assume that the photon transition probability is the same at the two sites, 1 and 2. [In glasses, this is known to be a poor approximation.[15] In such systems, the radiative lifetime which appears in our final expression for $J_1^{\rm eff}(E_1,r)$ should be the square root of the product of the individual radiative lifetimes.] Equation (A1) then reduces to the convenient form

$$|J_1^{\rm eff}(E_1,r)| = [V\kappa_1|I(\kappa_1)|/2\pi\hbar c r^2] \times |\langle 1|H_{\vec{k}}|1^*\rangle|^2 . \tag{A2}$$

Consider the radiative emission rate

$$\frac{1}{\tau_R} = \frac{2\pi}{\hbar}\sum_{\vec{k}} |\langle 1|H_{\vec{k}}|1^*\rangle|^2 (E_1 - \hbar\Omega_{\vec{k}}) = \frac{2\pi}{\hbar}\frac{V}{(2\pi)^3}\int_0^\infty 4\pi k^2\, dk\, |\langle 1|H_{\vec{k}}|1^*\rangle|^2 \times \frac{1}{\hbar c}\delta(k_1 - k) , \tag{A3}$$

where $\hbar c k_1 = E_1$. Simplifying,

$$1/\tau_R = (V/\hbar^2 c\pi) k_1^2 |\langle 1|H_{\vec{k}}|1^*\rangle|^2 . \tag{A4}$$

Comparing (A2) with (A4), we immediately find

$$|J_1^{\rm eff}(E_1,r)| = (\hbar/\tau_R)|I(\kappa_1)|/2\kappa_1 . \tag{A5}$$

This result is reproduced as (11) in the text.

---

*Work supported in part by the NSF and by the U. S. Office of Naval Research, Contract No. N00014-75C-0245.

[1]T. Holstein, S. K. Lyo, and R. Orbach, Phys. Rev. Lett. 36, 891 (1976).

[2]T. Holstein, S. K. Lyo, and R. Orbach, Phys. Rev. (to be published).

[3]T. Holstein, S. K. Lyo, and R. Orbach, Proceedings of the Colloque International du C.N.R.S., University of Lyon, 1976 (to be published).

[4]P. M. Selzer and W. M. Yen (private communication).

[5]T. Forster, Ann. Phys. (Paris) 2, 55 (1948); D. L. Dexter, J. Chem. Phys. 21, 836 (1953).

[6]It leaves out interference factors and those processes that involve phonon absorption and emission on different sites. See Ref. 3 for details.

[7]A. L. Schawlow, in *Advances in Electronics*, edited by J. R. Singer (Columbia U. P., New York, 1961), p. 50.

[8]R. Orbach, in *Optical Properties of Ions in Crystals*, edited by H. M. Crosswhite and H. W. Moos (Interscience, New York, 1967), p. 445.

[9]M. Blume, R. Orbach, A. Kiel, and S. Geschwind, Phys. Rev. 139, A314 (1965).

[10]I. S. Gradshteyn and I. M. Ryzhik, *Table of Integrals, Series, and Products* (Academic, New York, 1965).

[11]S. Geschwind, G. E. Devlin, R. L. Cohen, and S. R. Chinn, Phys. Rev. 137, A1087 (1965).

[12]Allan C. G. Mitchell and Mark W. Zemansky, *Resonance and Excited Atoms* (Cambridge U. P., Cambridge, England, 1961), p. 99.

[13]T. Holstein, Phys. Rev. 72, 1212 (1947).

[14]This approximation is discussed at some length by Jean-Pierre Barrat, J. Phys. Radium (1959). An abbreviated version has been published in J. Phys. (Paris) 20, 541 (1959); 20, 633 (1959); 20, 657, 657 (1959). The approximation amounts to taking each atom at the center of a sphere of radius d, and is more correct the larger the ratio $d/l(E)$.

[15]N. Motegi and S. Shionoya, J. Lumin. 8, 1 (1973).

[16]M. J. Weber, J. A. Paisner, S. S. Sussman, W. M. Yen, L. A. Riseberg, and C. Brecher, J. Lumin. 12, 729 (1976); C. Brecher and L. A. Riseberg, Phys. Rev. B 13, 81 (1976); M. J. Weber, Proceedings of the Colloque International du C.N.R.S., University of Lyon, 1976 (to be published).